Supporting information

Near-infrared Photothermal Conversion of Stable Radicals Photoinduced from a Viologen–based Coordination Polymer

*Shanshan Wang,[a] Shuning Li,[a] Junyu Xiong,[a] Zhengguo Lin,[a] Wei Wei[b] and Yanqing Xu *[a]*

a. Key Laboratory of Cluster Science, Ministry of Education of China, Beijing Key Laboratory of Photoelectronic/Electrophotonic Conversion Materials, School of Chemistry, Beijing Institute of Technology, Beijing 100081, P. R. China. E-mail: xyq@bit.edu.cn

b. Department of Chemistry, Capital Normal University, Beijing 100048, China.

1. General Method

All chemicals were purchased from commercial sources and used without further purification. NMR spectra were recorded with a Bruker Avance 400 MHz NMR spectrometer. Fourier transform infrared (FT-IR) spectra were obtained on a Nicolet 170SXFT-IR spectrophotometer in the range of 400–4000 cm^{-1} using KBr pellets. Powder X-ray diffraction (PXRD) patterns were collected on a Bruker instrument (D8 Venture) with graphite-monochromatized Cu Kα radiation (λ = 0.154 nm; scan speed = 2° min^{-1}; 2θ =5–50°) at room temperature. UV–vis diffuse reflectance spectra were recorded on a UV-2600 spectrometer (SHIMADZU) in the range 200-800 nm. Thermogravimetric analysis (TGA) were carried out on a Shimadzu DTG-60AH thermal analyzer under N_2 atmosphere at a heating rate of 10 °C min^{-1}. Elemental analyses were determined on an Elementar Vario ELIII analyzer. Electron paramagnetic resonance (EPR) was performed on a JEOL JES FA200 spectrometer with a 100 kHz magnetic field. X-ray photoelectron spectra (XPS) were recorded on a Thermo ESCALAB 250Xi spectrometer (Al Kα radiation). Quantum chemical computations were performed with the Gaussian 09 programs[1]. Geometry optimization calculations of the bpbc ligand were fully optimized with density functional theory (DFT) methods at the B3LYP/6-31G (d) level of theory. Frequencies calculations were also performed at the same level of theory to confirm that the optimized stable structures possess no imaginary frequency.

2. Synthesis of N,N'-bis(3-methyl-4-carboxylatophenyl)-4,4'-bipyridinium dihexafluorophosphate (*H_2bcbp·2PF_6*).

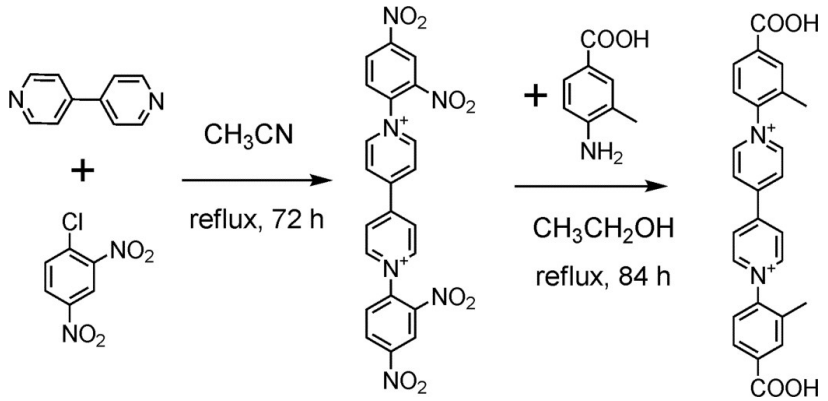

Scheme 1. Synthesis of H_2bcbp.

Ligand H_2bcbp·2Cl was prepared in the following two steps modified upon literature procedures.[2] For the first step as shown in the picture above, a solution of 4,4′-bipyridine (2.4 g, 15 mmol) and 2,4-dinitrochlorobenzene (9.1 g, 45 mmol) in acetonitrile (90 mL) was heated under reflux for 72 h. Then the hot mixture of the reaction was filtered, and washed with the right amount of ethanol for three times. The as-prepared solid product was dried under vacuum for 18 hours. As a result, the white solids of 1,1′-bis(2,4-dinitrophenyl)-(4,4′-bipyridinium) dichloride was collected and used without further purification (4.3 g, yield: 54%).

Secondly, 1,1′-bis(2,4-dinitrophenyl)-(4,4′-bipyridinium) dichloride (2.8 g, 5 mmol) and 4-amino-3-methylbenzoic acid (1.89 g, 12.5 mmol) were dispersed in 100 mL ethanol solution, and then heated under reflux for 96 h. After cooling to the room temperature, the formed brown solid of H_2bcbp·2Cl was collected by filtration, and recrystallized in water as dark yellow crystals (1.89 g; 82%).

KPF_6 (9.2 g, 0.05 mol) was added to *H_2bcbp*·2Cl (9.13 g, 0.02 mol) in 50 mL of distilled H_2O, and the mixture was stirred at 80 °C for 10 h. The resulting solid was collected by filtration, and washed with water for several times, then dried overnight at 80 °C in the vacuum (Yield: 93%). ^{1}H NMR (400 MHz, DMSO-d6): 9.62 (d, J=6.8 Hz, 4H), 9.084 (d, J=7.2 Hz, 4H), 8.194 (s, J=0.8 Hz, 2H), 8.121 (d, J=9.6, 2H), 7.885 (d, J=8.4 Hz, 2H), 2.292 (s, J=2.8 Hz, 6H). IR (KBr pellet, cm^{-1}): 3441(m), 3127(w), 3053(w), 2359(w), 1705(m), 1638(s), 1538(m), 1485(w), 1438(m), 1379(w), 1285(m), 1198(m), 1038(w), 831(s), 778(m), 558(s).

*3. Synthesis of **1**.*

H_2bcbp·2PF_6 (0.014g, 0.03mmol) and $La(NO_3)_3·6H_2O$ (0.043g, 0.1mmol) were mixed in CH_3CN/CH_3OH (1:1 v/v, 6 mL) and sonicated for 10 minutes. The resulting solution was kept in 120°C for 2 days in a teflonlined autoclave. The pale yellow crystals were obtained after cooling to room temperature at the speed of 2 °C h^{-1}. The as-prepared crystals **1** were washed by CH_3CN/CH_3OH (1:1 v/v) for several times to remove excess ligand powders, and then dried in air (Yield: 59% based on ligand). Elemental analysis calculated for C_{234} H_{288} La_{10} N_{42} $O_{127.5}$: C, 39.53; H, 4.08; N, 8.27.

Found: C, 39.13; H, 3.97; N, 8.21. IR (KBr pellet, cm^{-1}): 3414 (m), 3120 (w), 2426 (w), 2359 (w), 1626 (m), 1418 (s), 1392 (s), 1318 (m), 1198 (w), 1111 (w), 1032 (w), 838 (w), 785 (m), 724 (w), 658 (w), 464 (w).

4. X-ray crystallography.

Suitable single crystal of **1** was mounted on a glass fiber for the X-ray measurement. Diffraction data were collected on a Rigaku-AFC7 equipped with a Rigaku Saturn CCD area-detector system. The measurement was made by using graphite monochromatic Mo Kα radiation (λ= 0.71073 Å). The frame data were integrated, and absorption correction was calculated using the Rigaku CrystalClear program package. All calculations were performed with SHELXTL-97 program package,[3] and structures were solved by direct methods and refined by full-matrix least-squares fitting on F^2. All non-hydrogen atoms were refined anisotropically, and hydrogen atoms of the organic ligands were generated theoretically onto the specific atoms. The diffraction data of **1** was treated by the "SQUEEZE" method as implemented in PLATON to remove diffuse electron density associated with these severely disordered solvent molecules (PLAT990_ALERT_1_B). The partial site occupation and disorder of mononuclear $La(NO_3)_6^{3-}$ guest moieties lead to some alerts (PLAT307_ALERT_2_A, PLAT430_ALERT_2_A and PLAT430_ALERT_2_B) in checkcif report. High thermal motion of terminal NO_3^- in framework causes their large Ueq values compared with that of neighboring atoms, which is shown as alert level B (PLAT220_ALERT_2_B, PLAT241_ALERT_2_B and PLAT242_ALERT_2_B). The crystal data and the structure refinements are summarized in Table S1.

Table S1. Crystal data and structure refinements for **1**.

formula	$C_{26}\ H_{32}\ La_{1.1111}\ N_{4.6667}\ O_{14.1667}$
Mr.	790.90
Crystal system	trigonal
Space group	R 32

a [Å]	16.2731(5) Å
b [Å]	16.2731(5) Å
c [Å]	66.968(3) Å
V [A^3]	15358.14(120) Å^3
Z	18
D_{calcd} [g/cm^3]	1.5390
Measured refl.	56865
Unique refl.	8467
R_{int}	0.0482
GooF	1.048
R_1, wR_2 [I> 2σ(I)]	0.0460, 0.1265
R_1, wR_2 [all data]	0.0499, 0.1287

5. Calculation of photothermal conversion efficiency.

The conversion efficiency was determined according to previous method.[4-6] Details are as follows:

Based on the total energy balance for this system:

$$\sum_i m_i C_{pi} \frac{dT}{dt} = Q_s - Q_{loss}$$

where m_i (0.19 g) and $C_{p,i}$ (0.8 J (g ^{o}C)$^{-1}$) are the mass and heat capacity of system components (samples **1R** and quartz glass), respectively. Q_s is the photothermal heat energy input by irradiating NIR laser to sample **1R**, and Q_{loss} is thermal energy lost to the surroundings. When the temperature is maximum, the system is in balance.

$$Q_s = Q_{loss} = hS\Delta T_{max}$$

where h is heat transfer coefficient, S is the surface area of the container, ΔT_{max} is the maximum temperature change. The photothermal conversion efficiency η is calculated from the following eaquation:

$$\eta = \frac{hS\Delta T_{max}}{I\left(1 - 10^{-A_{808}}\right)}$$

where I is the laser power (1.5 W cm^{-2}) and A_{808} is the absorbance of the samples at the wavelength of 808 nm (0.143).

In order to obtain the hS, a dimensionless driving force temperature, θ is introduced as follows:

$$\theta = \frac{T - T_{surr}}{T_{max} - T_{surr}}$$

where T is the temperature of **1R**, T_{max} is the maximum system temperature (111.1 ^{o}C), and T_{surr} is the initial temperature (23.1 ^{o}C).

The sample system time constant τ_s

$$\tau_s = \frac{\sum_i m_i C_{p,i}}{hS}$$

thus $\frac{d\theta}{dt} = \frac{1}{\tau_s hS\Delta T_{max}} Q_s - \frac{\theta}{\tau_s}$

when the laser is off, $Q_s = 0$, therefore $\frac{d\theta}{dt} = -\frac{\theta}{\tau_s}$, and $t = -\tau_s \ln \theta$

so hS could be calculated from the slope of cooling time vs $\ln \theta$. Therefore, τ_s is 40.7 s (Fig. S10) and the photothermal conversion efficiency η is 77%.

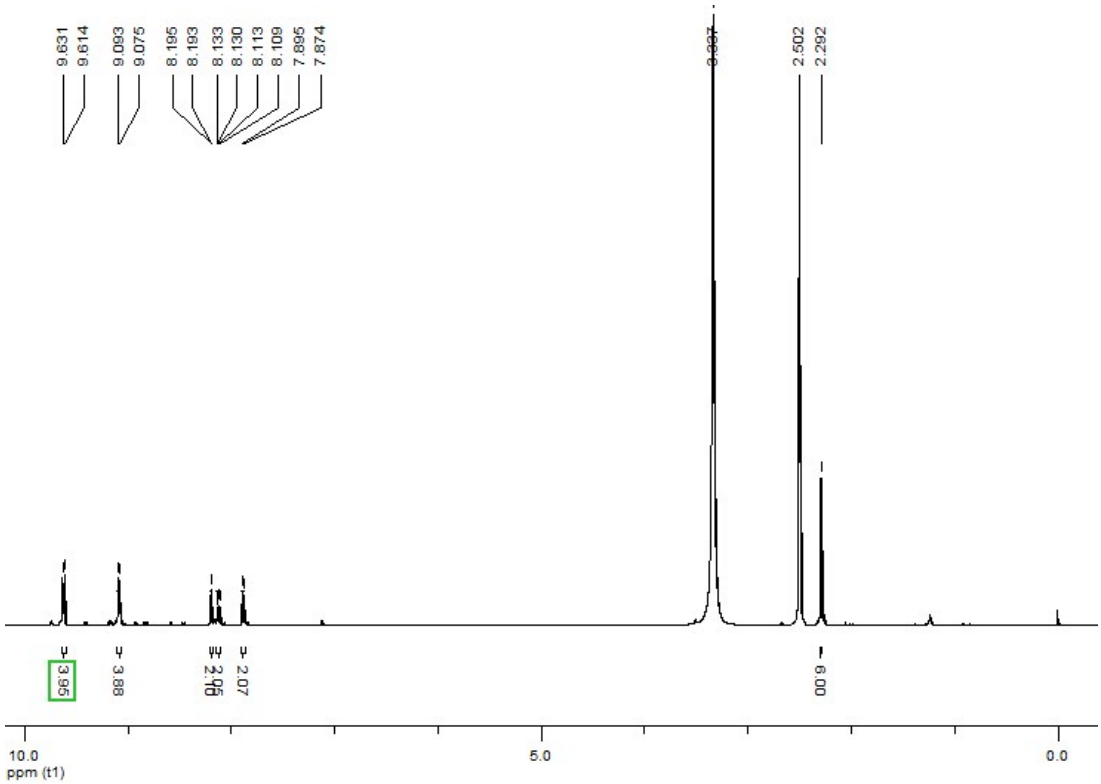

Fig. S1. The ^{1}H NMR of ligand H_2bcbp·2PF_6 (400 MHz, DMSO-d_6).

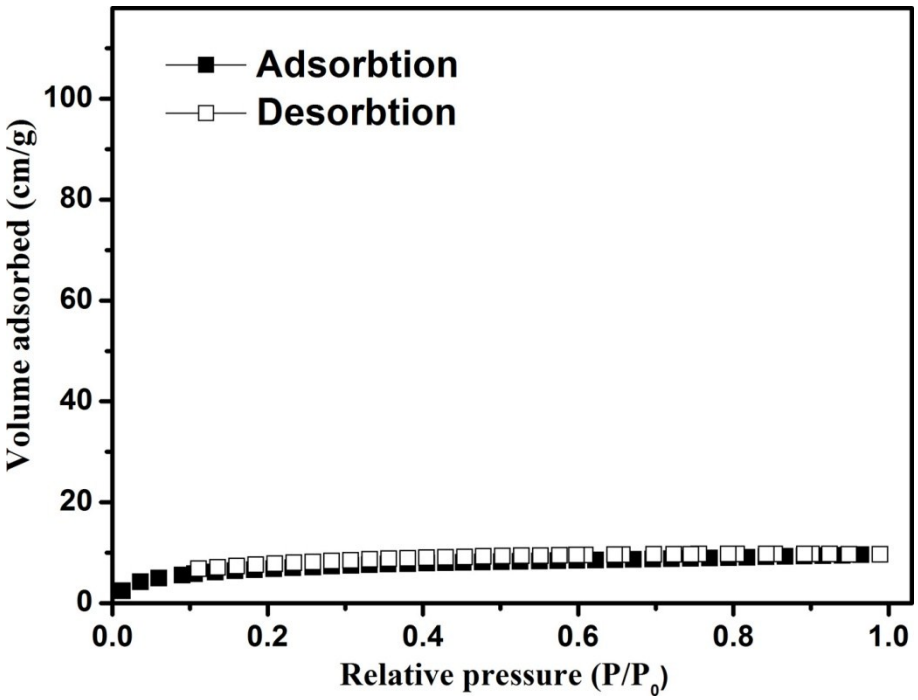

Fig. S2. N_2 adsorption-desorption isotherm of **1**.

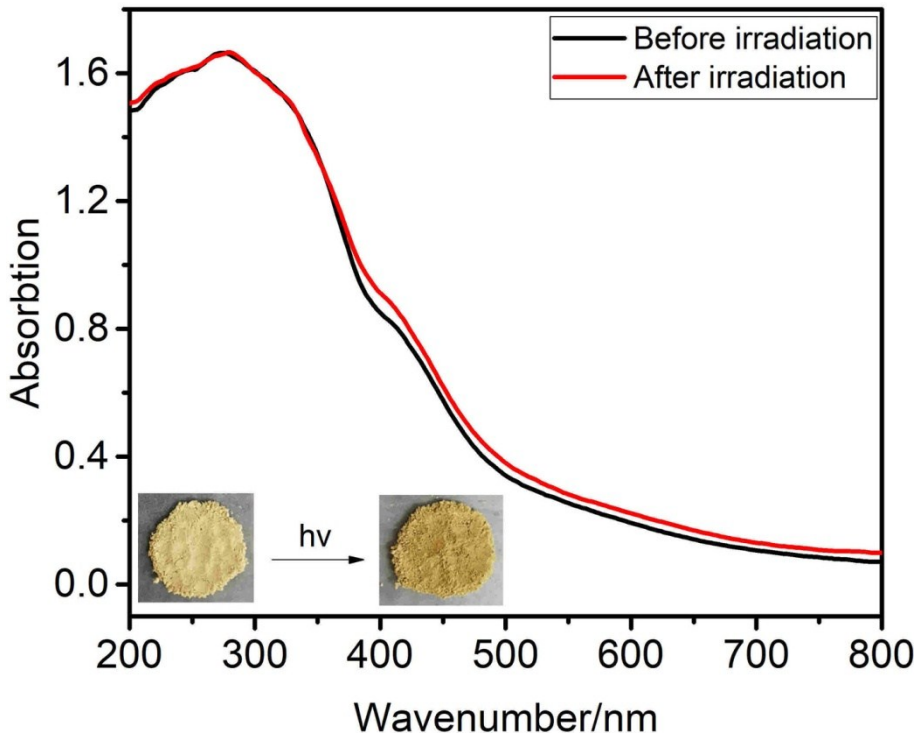

Fig. S3. UV-vis diffuse reflectance spectura and photographs showing the photochromic behaviors of ligand H_2bcbp·$2PF_6$.

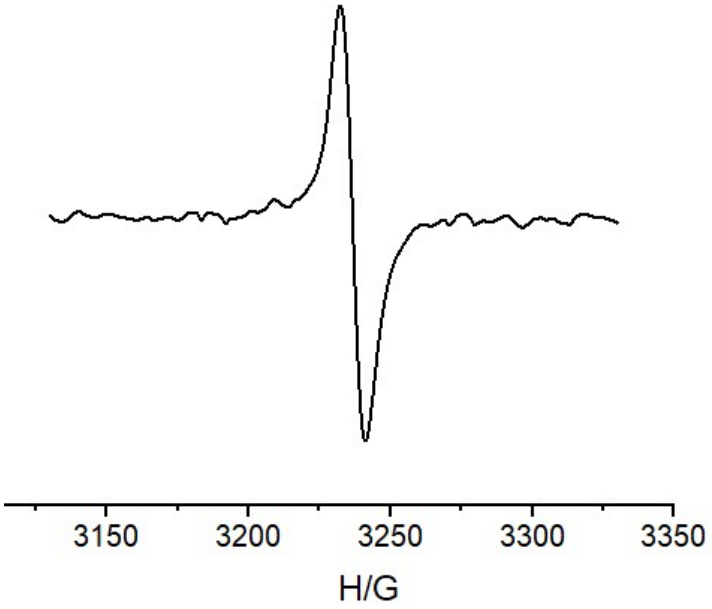

Fig. S4. EPR spectrum of ligand H_2bcbp·2PF_6 after irradiation.

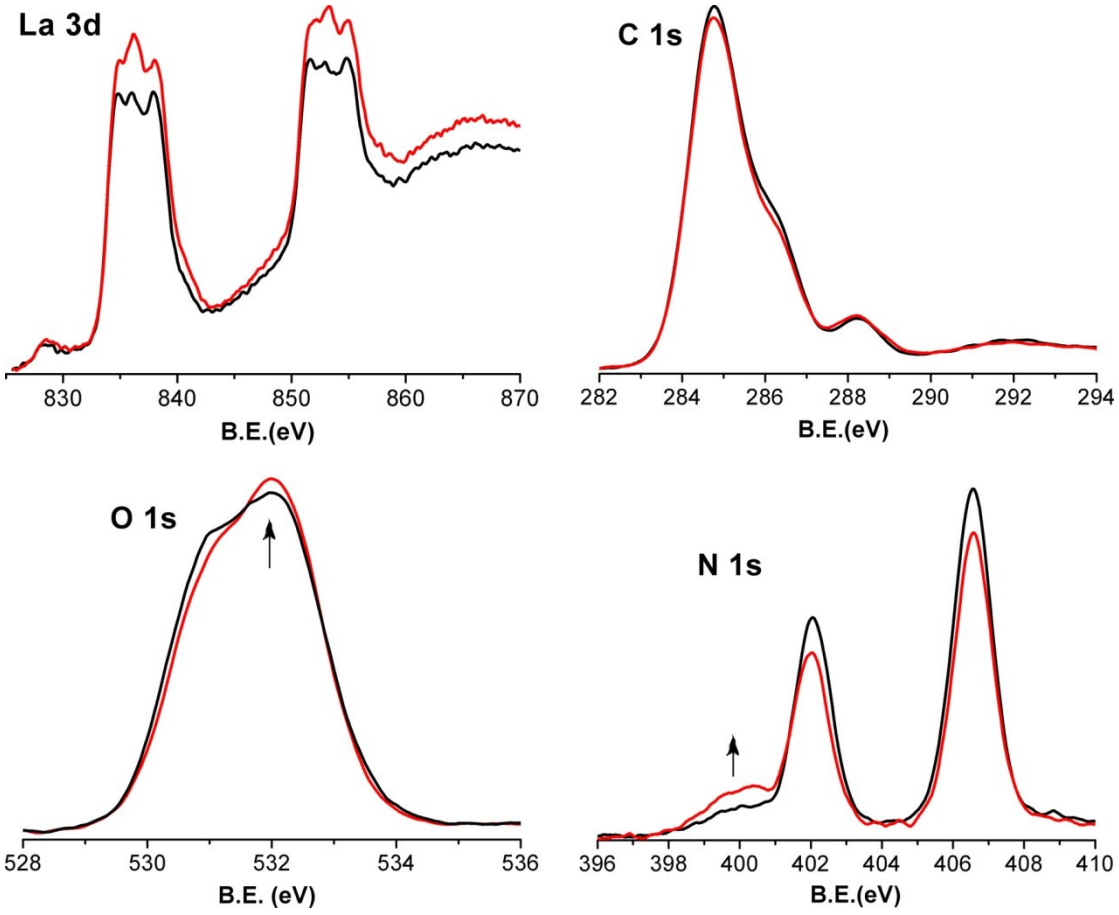

Fig. S5. High-resolution XPS spectra of sample before and after irradiation.

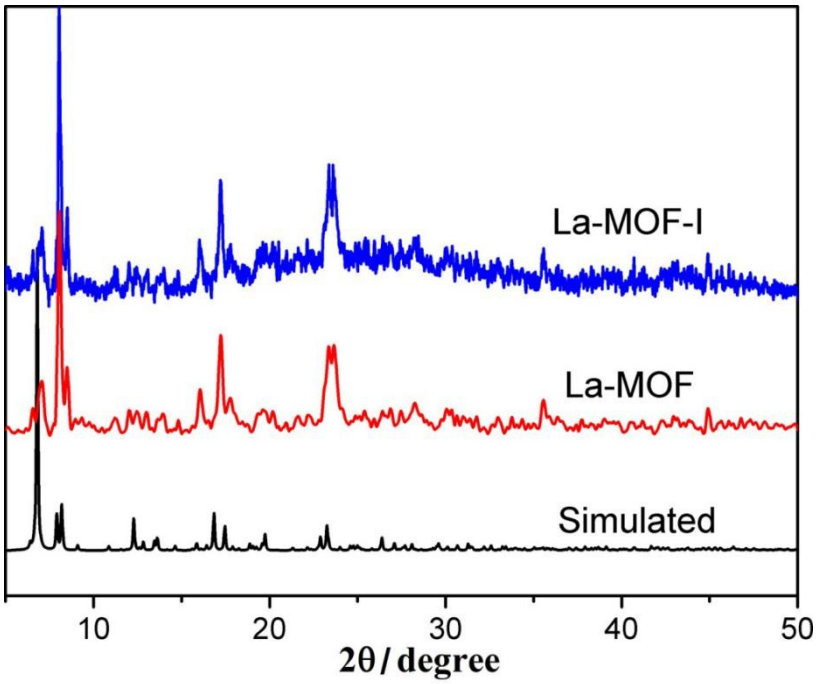

Fig. S6. Powder XRD patterns of **1** and **1R**.

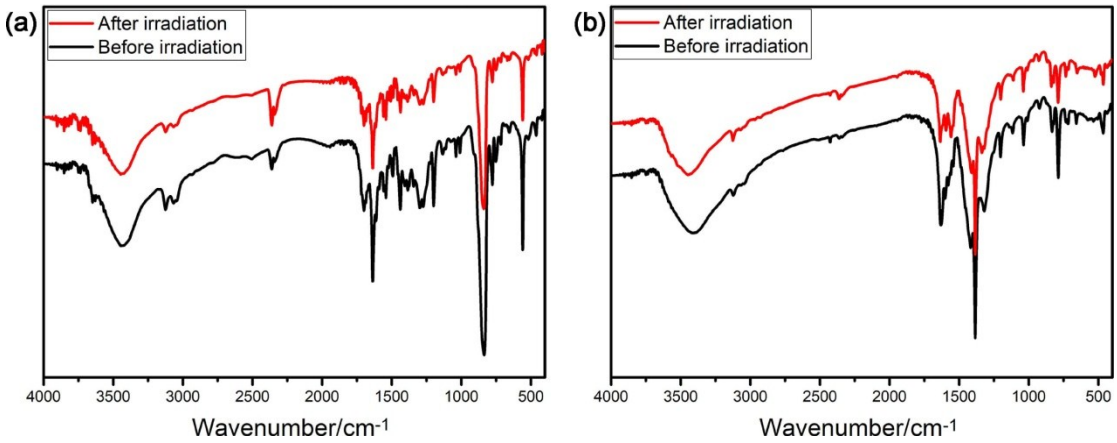

Fig. S7. IR spectra of (a) ligand H_2bcbp·2PF_6 and (b) **1** before and after irradiation.

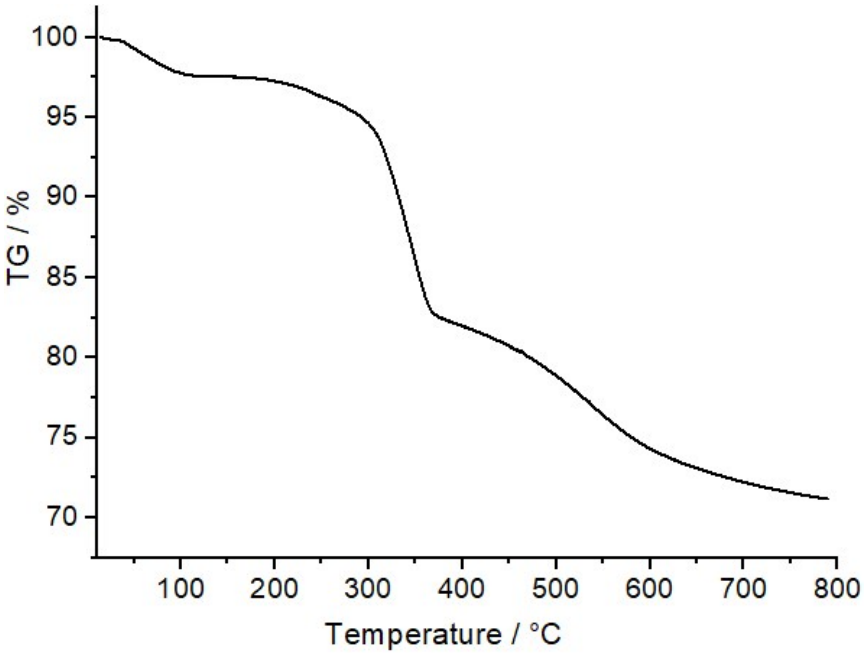

Fig. S8. Thermogravimetric analysis of **1**.

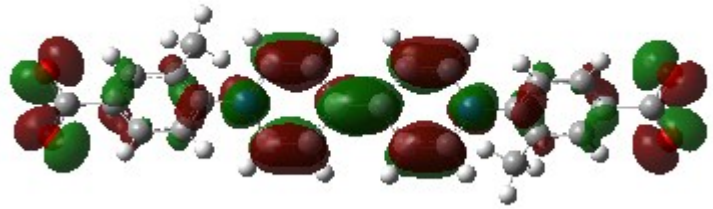

LUMO

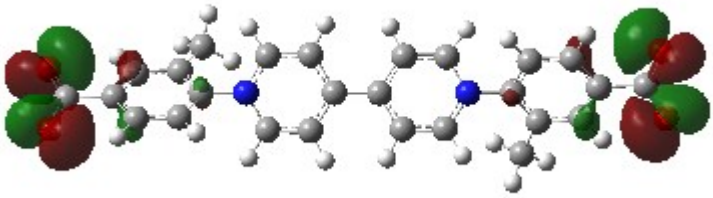

HOMO

Fig. S9 The HOMO and LUMO sets for neutral ligand bcbp possibly implying phtoinduced eletron transfer mainly from the carboxy group to the pyridinum cation.

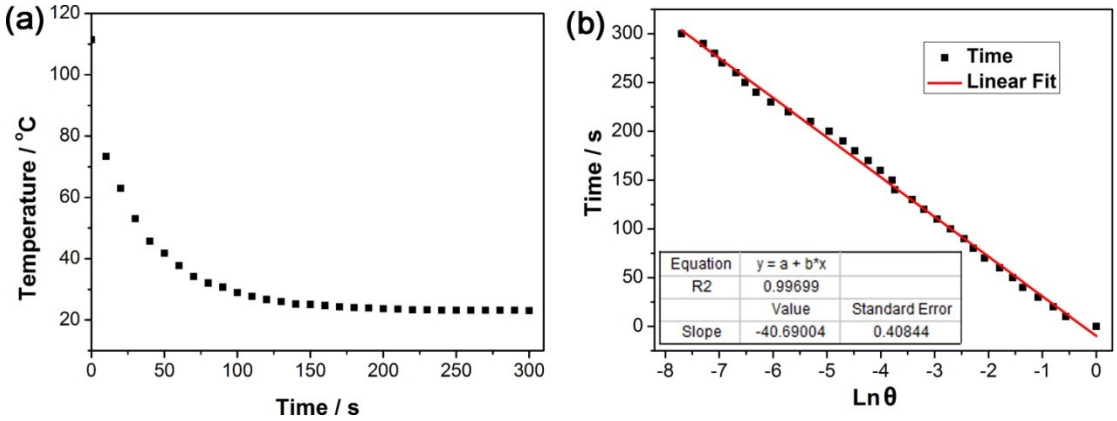

Fig. S10. The cooling curve of **1R** film after irradiation with 808 nm laser (1.5 W cm^{-2}) (a) and its corresponding time-lnθ linear curve (b).

References:

1. M. J. Frisch, G.W.T., H. B. Schlegel, G. E. Scuseria, M. A. Robb, J. R. Cheeseman, G. Scalmani, V. Barone, G. A. Petersson, H. Nakatsuji, X. Li, M. Caricato, A. Marenich, J. Bloino, B. G. Janesko, R. Gomperts, B. Mennucci, H. P. Hratchian, J. V. Ortiz, A. F. Izmaylov, J. L. Sonnenberg, D. Williams-Young, F. Ding, F. Lipparini, F. Egidi, J. Goings, B. Peng, A. Petrone, T. Henderson, D. Ranasinghe, V. G. Zakrzewski, J. Gao, N. Rega, G. Zheng, W. Liang, M. Hada, M. Ehara, K. Toyota, R. Fukuda, J. Hasegawa, M. Ishida, T. Nakajima, Y. Honda, O. Kitao, H. Nakai, T. Vreven, K. Throssell, J. A. Montgomery, Jr., J. E. Peralta, F. Ogliaro, M. Bearpark, J. J. Heyd, E. Brothers, K. N. Kudin, V. N. Staroverov, T. Keith, R. Kobayashi, J. Normand, K. Raghavachari, A. Rendell, J. C. Burant, S. S. Iyengar, J. Tomasi, M. Cossi, J. M. Millam, M. Klene, C. Adamo, R. Cammi, J. W. Ochterski, R. L. Martin, K. Morokuma, O. Farkas, J. B. Foresman, and D. J. Fox, Gaussian 09, Revision A.02; Gaussian, Inc.: Wallingford, CT, 2009. , 2009
2. F. Lin, T. G. Zhan, T. Y. Zhou, K. D. Zhang, G. Y. Li, J. Wu, X. Zhao, *Chem Commun.*, 2014, 50, 7982-7985.
3. G. M. Sheldrick, SHELXL-97, Program for Solution of Crystal Structures, University of Göttingen, Göttingen, Germany, 1997.
4. B. Kim, H. Shin, T. Park, H. Lim, E. Kim, *Adv. Mater.*, 2013, 25, 5483-5489.
5. Y. Wang, W. Zhu, W. Du, X. Liu, X. Zhang, H. Dong, W. Hu, *Angew. Chem. Int. Ed.*, 2018, 57, 3963 –3967.
6. B. Lü, Y. Chen, P. Li, B. Wang, K. Müllen, M. Yin, *Nat. Commun.*, 2019, 10, 767.

`